

SCIENTIA  
IRANICA

Sharif University of Technology

Scientia Iranica

Transactions D: Computer Science &amp; Engineering and Electrical Engineering

<http://scientiairanica.sharif.edu>

# Towards green data center microgrids by leveraging data center loads in providing frequency regulation

W. Qi and J. Li<sup>1,\*</sup>

Department of Electrical and Computer Engineering, Clarkson University, Potsdam, 13699, NY, USA.

Received 1 May 2019; accepted 20 October 2019

## KEYWORDS

Data center;  
Microgrid;  
Load frequency control;  
Primary frequency control;  
Demand response.

**Abstract.** In an electricity grid, imbalance between generation and load should be corrected within seconds so that frequency deviations will not threaten the stability and security. This is especially important for a low-inertia microgrid operated in islanded mode, which is equipped with a limited number of synchronous generators in regulating frequency. To this end, in data center microgrids with limited on-site generators and increased green energy, when isolated from the utility grid, frequency deviation due to generation-load imbalance could be corrected by conventionally generating units as well as data center loads. Focusing on high PV penetrated data center microgrid operated in islanded mode, this paper explores effective control strategies for data center loads to participate in primary frequency response. By analyzing unique operational characteristics of traditional and PV generation units and Uninterruptible Power Supply (UPS) units as well as power consumption characteristics of IT components and cooling systems, the proposed load control strategy design effectively utilizes primary FR capabilities while not compromising data center Quality of Service (QoS) requirements. Numerical simulations via MATLAB/Simulink illustrated effectiveness of the proposed load control strategy in enhancing renewable energy penetration without compromising system stability and security, providing a viable solution for future green data centers.

© 2019 Sharif University of Technology. All rights reserved.

## 1. Introduction

The rapid growth in the need for data processing, storage, and communication leads to the proliferation of data centers that consist of (tens of) thousands of servers. The operation of such data centers requires extensive electric energy consumption. According to the Lawrence Berkeley National Laboratory (LBNL) report [1], data centers in the U.S. consumed over 70

billion kWh of electricity in 2014. Currently, data centers consume up to 3% of the global electricity production and produce 200 million metric tons of CO<sub>2</sub> emission annually [2]. Indeed, it is projected that by 2030, data centers in the U.S. could consume up to 20% of electricity production, emerging as a new “polluter” with significant environmental impacts. Accordingly, high electricity bills and serious environmental concerns have drawn the attention of many researchers to data center energy efficiency [3–7]. Specifically, some previous researches recommended using microgrids to provide electricity supply for data centers by integrating onsite renewables and energy storages to guarantee high power quality, reliability, and sustainability requirements [3–5].

Data center microgrids can operate in both grid-connected and islanded modes. Grid-connected data

1. Present address: Department of Electrical and Computer Engineering, Rowan University, Glassboro, 08028, NJ, USA.

\*. Corresponding author. Tel.: +1 856 256-5345  
E-mail addresses: [qiw@clarkson.edu](mailto:qiw@clarkson.edu) (W. Qi);  
[lijie@rowan.edu](mailto:lijie@rowan.edu) (J. Li)

center microgrids receive frequency support from the main grid. On the other hand, when operated in islanded mode, data center microgrids must maintain the frequency and voltage stability by itself. If high penetration of renewable generation, such as PV, is integrated into the data center microgrid, uncertain power supply and volatile data center workload may induce severe real-time generation-load imbalance. This could lead to excessive system frequency deviations and threaten the stability and security of data center electricity supply system [8]. Therefore, proper frequency regulation strategies are required for the stable operation of data center microgrid with increased renewable generation integration [9].

In islanded microgrids, the frequency deviation induced by load changes is usually corrected by adjusting power output of the traditional generating units, which is referred to as primary frequency control [10]. However, in the future data center microgrids with increased penetration of renewables to pursue “green data center” objectives, system inertia and frequency response capabilities are greatly reduced and it becomes more expensive and technically difficult to perform such primary frequency control. Thus, researches [11,12] have recommended the use of Energy Storage Systems (ESSs) to achieve frequency regulation of microgrids. However, this comes with two issues: (i) Installing ESSs in a microgrid may not be economically efficient, and (ii) Life span of ESSs could be severely compromised due to frequent charging-discharging cycles to provide frequency regulation. Therefore, designing proper load control strategy to support frequency regulation in microgrids is receiving greater attentions [13-15].

Indeed, electrical loads of a data center represent good frequency response capabilities through effective load control. Electric loads of a data center microgrid are classified into two major categories: IT equipment loads (e.g., storage devices as well as processing and computing server machines) that normally consume about 36% data center energy, and cooling system loads (e.g., fans, air handlers, chillers, etc.) that usually consume about 50% data center energy [16]. IT equipment is mainly used to process two types of data center workloads, namely delay-sensitive and delay-tolerant tasks. To this end, flexibilities of the IT equipment in processing delay-tolerant tasks and the cooling system in maintaining specific temperature range could be leveraged to control power consumption of data center over different time periods and, in turn, regulate frequency of the data center microgrid.

This paper explores effective design and implementation of load frequency control in a data center to support the microgrid system primary frequency regulation with increased PV integration. Specifically, unique characteristics of cooling and IT loads in a data

center will be analyzed to quantify their primary frequency regulation capabilities while not compromising data center Quality of Service (QoS) requirements. To this end, we first use MATLAB/Simulink to build a data center microgrid simulation platform for simulating traditional diesel generation units, PV generation, Uninterruptible Power Supply (UPS), and power consumption model of the data center (IT components and cooling system) while considering characteristics of the data center electrical loads. Then, we propose an electric load control strategy to support primary frequency regulation of data center microgrid in islanded mode and verify its effectiveness in maintaining system frequency in comparison with the situation that primary regulation is only provided on the generation side. Finally, the impacts of communication and actuation latency of data center load controllers as well as the actual response time of data center electric loads to such control signals on the overall performance of frequency regulation are analyzed.

The rest of the paper is organized as follows. Section 2 introduces models of major components of a typical data center microgrid. Section 3 presents the detailed control strategy for data center electric loads participating in primary frequency regulation. Numerical studies are presented in Section 4. Finally, conclusions and future research directions are drawn in Section 5.

## 2. Simulation of a data center microgrid

A typical data center microgrid consists of traditional diesel generating units, renewable generation units such as PV, Automatic Transfer Switch (ATS), switchgear, UPS, Power Distribution Units (PDUs), and data center electric loads (including both IT and cooling loads), as shown in Figure 1.

### 2.1. Diesel generating unit

Two diesel generating units equipped with speed governor and excitation system are simulated. The diesel units are directly connected to the main bus of the data center designed to provide primary frequency and voltage support as grid-forming units in islanded mode.

Figure 2 shows  $P - f$  and  $Q - V$  droop characteristics of the diesel units. Active power output of

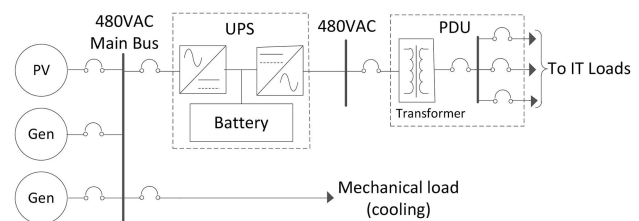
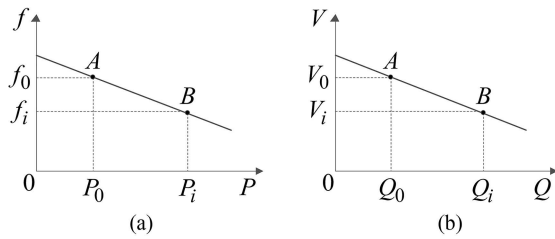


Figure 1. Representative diagram of data center microgrid [15].



**Figure 2.** Droop characteristics: (a)  $P - f$ , and (b)  $Q - V$ .

the diesel unit is predominately coupled with terminal frequency, while the reactive power output is mainly dependent on its terminal voltage magnitude. When frequency  $f$  is reduced from point  $A$  to point  $B$ , the droop control scheme will increase real power output  $P$  of the unit. Similarly, when the voltage magnitude  $V$  decreases from point  $A$  to point  $B$ , reactive power output  $Q$  of the unit increases.

**2.2. PV generating unit**

Renewable PV unit is simulated in our data center microgrid. The equivalent circuit of a PV cell is shown in Figure 3(a), which includes light-generated current source  $I_{ph}$ , a diode  $D$ , a shunt resistance  $R_{sh}$ , and a series resistance  $R_s$ . Figure 3(b) illustrates the

$I_{PV} - V_{PV}$  and  $P_{PV} - V_{PV}$  characteristics of a PV array. We can see that there is a maximum power point on the  $P_{PV} - V_{PV}$  curve. The Maximum Power Point Tracking (MPPT) module is usually utilized to extract the maximum available power from a PV array.

As shown in Figure 4, a PV array is connected to the main bus of the data center microgrid through a boost converter and a controllable inverter. The boost converter is regulated by MPPT control and the inverter is regulated by PQ (active power and reactive power) control. Since PV generation units are usually designed as grid-following units, the reference frequency  $f$  of a PV unit must be taken from the main bus of the data center microgrid by a Phase Lock Loop (PLL).

**2.3. Uninterruptible Power Supply (UPS)**

UPS systems are a crucial part of a data center microgrid, especially in the occasions that critical equipment must be protected from any potential power quality issues and power supply outage is not tolerable. Online UPS (as shown in Figure 5) can provide the highest level of protection against any potential power outage and quality problems, such as transients as well as

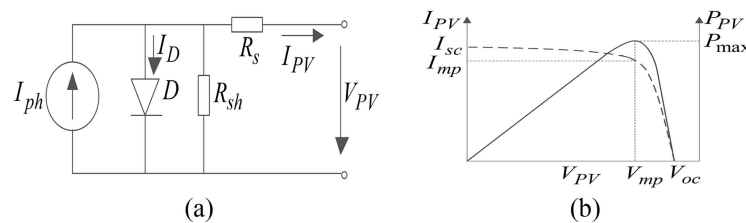


**Figure 3.** PV cell: (a) Equivalent circuit, and (b)  $I_{PV} - V_{PV}$  and  $P_{PV} - V_{PV}$  characteristics.

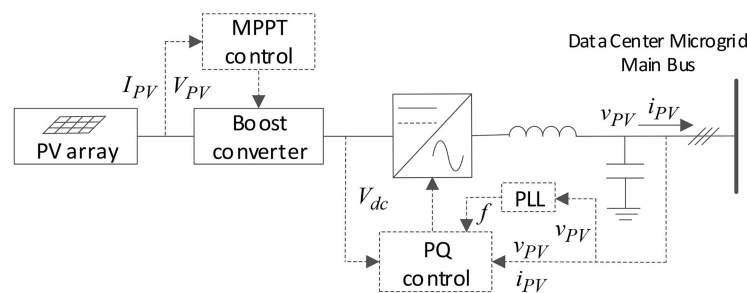


**Figure 4.** Control structure of PV cell.

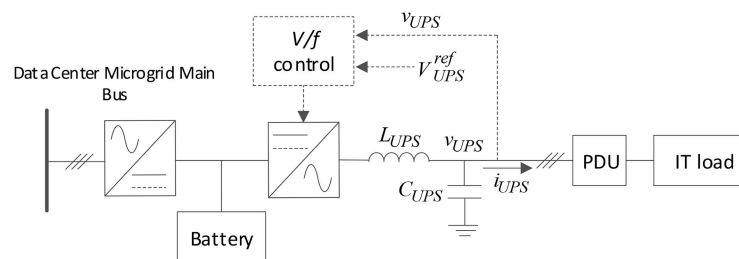


**Figure 5.** Control structure of a UPS.

voltage sags and swells. AC power flowing through the UPS is converted to DC power of which a portion charges the battery and the rest is inverted back to AC power for the connected equipment. The double conversion process essentially prevents power events, such as power fluctuations, power outages, and power surges, from reaching the equipment, thus yielding a preferable protection level.

UPS systems are normally designed to provide short-term power supply for data center equipment when electric outage happens so as to give data center enough time to activate onsite backup generators. The size of the UPS battery bank is determined by the required time duration of power supply for the data center, which typically varies from 2 ~ 3 min to 7 ~ 10 min [17]. In our data center model, the lead-acid battery is considered, which can provide 5-minute power supply to the data center.

**2.4. Data center load**

Power consumption of a data center mainly occurs in its IT components and cooling system [18]. As shown in Figure 6, IT components include router clusters, Hard Disk Drive (HDD) clusters, and server clusters; cooling system consists of fans, Computer Room Air Handlers (CRAHs), and chillers [19,20]. IT components in a data center are usually divided into exclusive groups for handling different IT services, including data processing, computing, and storage tasks. That is, each component is assigned processing a unique type of IT services. In this study, we consider that all devices, processing the same type of services, are operated homogeneously, i.e., at the same frequency and power level.

1. *Component power consumption.*

Three types of IT services that are widely provided by data centers across the world are considered, including storage, processing, and computing. These services are further classified into two categories based on their distinct characteristics: delay-sensitive tasks and delay-tolerant tasks. Delay-sensitive means that a task must be processed immediately without delay, while delay-tolerant

tasks are batch jobs that can be completed within relatively loose deadlines. In this paper, storage and processing services are considered as delay-sensitive tasks and computing services are considered as delay-tolerant tasks [19].

- *Storage service:* Two groups of data center component clusters, HDD clusters, and router clusters are mainly used to provide storage services for upload and download actions. In this paper, power consumptions of HDD clusters and router clusters are formulated as linear functions of the task rate by Eq. (1);
- *Processing service:* A processing service involves server, HDD, and router component clusters. Power consumptions of the HDD and router clusters can be similarly simulated by Eq. (1). Server clusters could be operated under a set of discrete CPU frequency levels and a certain level will be selected depending on the upcoming workloads as well as the quality of service requirements. Eq. (2) calculates the power consumption of a server cluster, which includes power consumption related to the idle status, the server frequency  $f$ , and utilization.
- *Computing service:* A computing service is simulated as a delay-tolerant task in this paper. This task only involves server clusters and the power consumption is formulated in Eq. (3). Some computing tasks have pre-specified total execution time, measured in terms of the number of computing hours with a single-cluster capability. That is, tasks assigned to the data center should be completed within specified delay-tolerant time periods. Eq. (4) guarantees that all computing tasks will be completed.

$$P_{i,t} = \frac{\lambda_{i,t}}{\lambda_i^{\max}} \cdot P_i^{\max}, \quad i \in T^{DS}, \tag{1}$$

$$P_{i,t} = B_i \cdot I_{i,t} + A_i \cdot (f_{i,l,t})^3 \cdot \frac{\lambda_{i,t}}{\lambda_i^{\max}}, \quad i \in T^{DS}, \tag{2}$$

$$P_{i,t} = P_i^{\max} \cdot I_{i,t}, \quad i \in T^{DT}, \tag{3}$$

$$\sum_{t=1}^{NT} \sum_{i=1}^{Ncom} I_{i,t} = DTT, \tag{4}$$

$$P_t^{IT} = \sum_{i=1}^{Ncluster} P_{i,t}, \tag{5}$$

where  $i$ ,  $l$ , and  $t$  are indices of IT cluster, CPU frequency level, and time period. Decision variables include power consumption of IT component cluster  $P$  (kW), server frequency  $f$

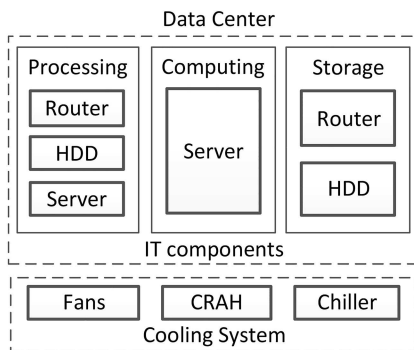


**Figure 6.** Component clusters of a data center.

(GHz), and commitment of a component cluster  $I$ . Parameters include the number of cloud services per unit task arriving at an IT cluster,  $\lambda$ ; power coefficient of a server cluster  $A$  and  $B$  (kW/GHz<sup>3</sup>, kW); Delay-Tolerant Task time requirement,  $DTT$  (seconds); number of computing clusters,  $N_{com}$ ; number of IT clusters,  $N_{cluster}$ ; total time period,  $NT$  (seconds); maximum power level of an IT cluster,  $P^{\max}$  (kW); set of delay-sensitive tasks,  $T^{DS}$ ; set of delay-tolerant tasks,  $T^{DT}$ ; and maximum capacity of an IT component cluster,  $\lambda^{\max}$  (tasks/s).

The total power consumption of all IT clusters is calculated by Eq. (5).

2. *Cooling system power consumption.*

Generally, the cooling system of a data center consists of fans, Computer Room Air Handlers (CRAHs), and water chiller. IT clusters are cooled with cold air at temperature  $T_{in}$ , which is drawn through the chassis by fans and expelled at temperature  $T_{out}$ . Hot air returns through a CRAH, where heat is removed and cooled to the cold air. CRAHs exchange the removed heat with a chilled water loop with cold water at temperature  $T_{water}$ . Finally, the cold water loop temperature is maintained by a chiller and cooling tower, which expels data center heat out [20].

Since all the heat generated by data center servers must be removed by air cooling, the thermodynamics of cooling the IT clusters can be captured by Eq. (6) [20]:

$$k \cdot C \cdot M_{i,t} \cdot T_{out} = P_{i,t} + k \cdot C \cdot M_{i,t} \cdot T_{in},$$

$$i \in \{T^{DS}, T^{DT}\}, \quad (6)$$

where  $P_{i,t}$  is the rate of heat removal (W) equal to the power withdraw of the IT clusters to maintain stable temperature,  $k$  is the containment index,  $M_{i,t}$  is the mass flow rate of air through the IT cluster (kg/s), and  $C$  is the specific heat capacity of air (J/g-k).

- *Fan:* The required flow rate through an IT cluster is achieved by forced air provided by the fans in this cluster. Fan power varies cubically with respect to the flow rate of air pushed (or sucked) by the device. Since flow rate varies linearly with respect to fan speed, the power consumption of fans in an IT cluster is calculated via Eq. (7):

$$P_{i,t}^F = P_i^{F,\max} \cdot (M_{i,t} / M_i^{F,\max})^3,$$

$$i \in \{T^{DS}, T^{DT}\}, \quad (7)$$

where  $P^{F,\max}$  is the maximum power of fan (kW)

and  $M^{F,\max}$  is the maximum flow rate through an IT cluster (cubic foot/minute).

The total power of all fans in the system can be calculated by Eq. (8):

$$P_t^{F,tot} = \sum_{i=1}^{N_{cluster}} P_{i,t}^F. \quad (8)$$

- *CRAH:* The total heat removed by all CRAHs is equal to the aggregate power consumption of all IT clusters, as described in Eq. (9). In addition, the amount of heat removed by a CRAH from the air can be calculated via Eq. (10).

$$\sum_{j=1}^{N_{crah}} Q_{j,t} = P_t^{IT}, \quad (9)$$

$$Q_{j,t} = EkC M_j v_j^{0.7} [k T_{out} + (1-k) T_{in} - T_{water}],$$

$$j \in CRAH. \quad (10)$$

In Eq. (10),  $E$  is heat transfer efficiency of the air,  $M_j$  represents the mass flow rate of the CRAH, and  $v_j$  is the fractional fan speed of the CRAH (from 0 to 1), which is used to calculate the power requirement to run the CRAH itself, as given in Eq. (11).

$$P_{j,t} = P_j^{idle} + P_j^{dyn} \cdot v_j^3, \quad j \in CRAH. \quad (11)$$

In Eq. (11),  $P^{idle}$  is idle power draw of CRAH (kW);  $P^{dyn}$  is dynamic power drawn by CRAH, which is equal to maximum power of the CRAH minus idle power; and  $v$  can be achieved by solving Eqs. (9) and (10).

The total power consumption of all CRAHs in the system is given in Eq. (12).

$$P_t^{CRAH,tot} = \sum_{j=1}^{N_{crah}} P_{j,t}. \quad (12)$$

- *Chiller:* The chiller accounts for the majority of the overall cooling power consumption in most data centers. In our data center microgrid, we consider a chiller capable of removing 2MW of heat with a peak power consumption of 1.2MW in maximum loading. The power model of the chiller is a function of total data center utilization (kW), as shown in Eq. (13), which can be derived from empirical regression curves [21].  $U_t$  is total data center utilization.

$$P_t^{chiller} = 185.7 \cdot U_t^2 + 461.2 \cdot U_t + 538.7. \quad (13)$$

The total power consumption of the entire cooling system is calculated by Eq. (14).

$$P_t^{cool} = P_t^{F,tot} + P_t^{CRAH,tot} + P_t^{chiller}. \quad (14)$$

### 3. Data center load control strategy

In this paper, load control refers to the adjustment of a proportion of the data center cooling and/or IT loads to the microgrid frequency deviation, providing the frequency regulation capabilities similar to those of generators. To this end, both the active power output of traditional generating units and power consumption of controllable cooling and IT loads will be regulated quickly to balance power supply and demand so as to restore the system frequency. This process is implemented in the primary frequency control of a data center microgrid.

In a data center microgrid with proliferated PVs, a sudden decrease in PV generation can lead to frequency drop of microgrid and terminal voltage swells of IT equipment, while a rapid increase in PV generation can result in rise in bus frequency and terminal voltage sags of IT equipment. Since IT equipment in data centers is very sensitive to large variations of frequency and voltage in the power supply, poor power quality can affect the performance of IT servers and even lead to property damage [22,23]. In addition, serious voltage and frequency variations might lead to unstable microgrid operation. Thus, over- or under-frequency protection devices are usually utilized to shut down IT equipment and/or cooling system. However, the variations will affect the QoS of data center services and economic benefits. To this end, an effective load control strategy to mitigate frequency and voltage fluctuations is a considerable option, especially when noting the increased penetration of renewables in future green data centers.

Frequency is regulated based on the measurement of frequency deviation. The load controller is triggered once the system frequency deviation exceeds a certain threshold and the frequency deviation time is larger than the actuation delay (latency)  $T_{Delay}$ . The actuation delay  $T_{Delay}$  consists of three parts: the computational time, the communication time, and the controller actuation time [14,24].

The data center cooling and IT loads can be changed instantaneously by ON/OFF command signals. In this paper, the primary control goal is to maintain the system frequency deviation within 0.5 Hz. When a frequency deviation in a disturbance exceeds the threshold, the load controller will be activated to regulate frequency by adjusting controllable loads (cooling and IT). The frequency, measured at the Point of Common Coupling (PCC) of the data center microgrid, is the input to the controller.

The procedure of the proposed load controller is shown in Figure 7. When system frequency is higher than the nominal value plus a threshold  $\Delta f_{th}$ , a portion of responsive cooling and IT loads (which were originally OFF) will be activated. In this occasion, IT loads will have higher priority to be activated, because processing more IT loads can bring higher benefits to the owner of the data center. On the other hand, when system frequency is lower than the nominal value minus a threshold  $\Delta f_{th}$ , a portion of the responsive cooling loads (which were originally ON) will be turned off. In this case, cooling loads will have higher priority for the same reason.

The above procedure is adaptive to various levels

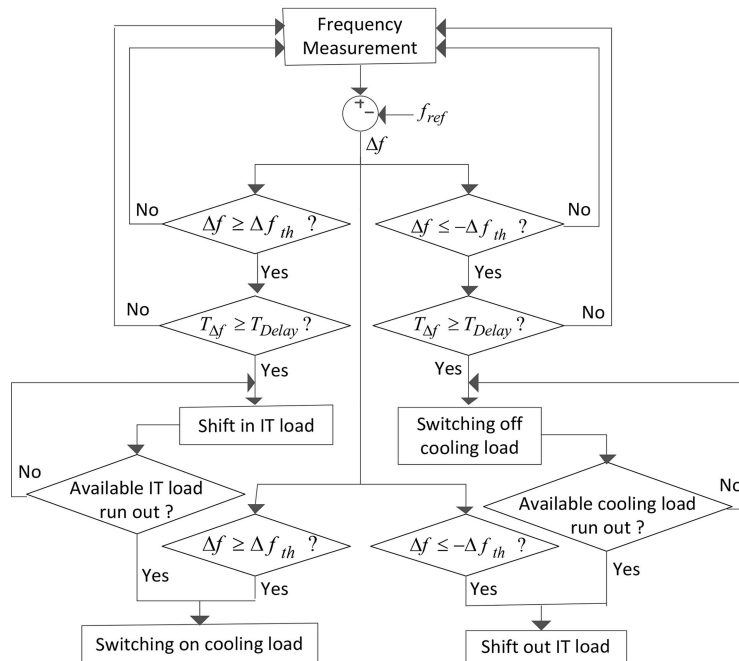


Figure 7. Data center load control strategy.

**Table 1.** Shedding behavior of cooling loads with 1 MW PV.

Stage	$\Delta f$ threshold	Cooling load regulation ratio
1	-0.05 Hz	10%
2	-0.1 Hz	20%

**Table 2.** Adding behavior of IT loads with 1 MW PV.

Stage	$\Delta f$ threshold	IT load regulation ratio
1	+0.05 Hz	10%
2	+0.1 Hz	20%

**Table 3.** Shedding behavior of cooling loads with 4 MW PV.

Stage	$\Delta f$ threshold	Cooling load regulation ratio
1	-0.02 Hz	10%
2	-0.04 Hz	20%
3	-0.06 Hz	30%
4	-0.08 Hz	40%
5	-0.1 Hz	50%
6	-0.12 Hz	60%
7	-0.14 Hz	70%
8	-0.16 Hz	80%
9	-0.18 Hz	90%
10	-0.2 Hz	100%

**Table 4.** Shedding behavior of IT load with 4 MW PV.

Stage	$\Delta f$ threshold	IT load regulation ratio
1	-0.22 Hz	10%
2	-0.24 Hz	20%
3	-0.26 Hz	30%
4	-0.28 Hz	40%
5	-0.3 Hz	50%
6	-0.32 Hz	60%

of frequency deviation thresholds and load regulation proportions, as shown in Tables 1-4. This setup is to be tuned based on system specifications in order to effectively utilize the available load regulation capabilities for mitigating frequency deviations. For instance, comparing Tables 3-6 with Tables 1 and 2, when PV penetration is higher, PV power output uncertainty could be more significant and would induce larger frequency deviation. In turn, more load control capabilities are expected for frequency regulation. The impact of actuation delay (latency),  $T_{Delay}$ , is considered by switching ON/OFF of cooling load actuation delay at 80 ms/20 ms and switching ON/OFF of IT load actuation delay at 120 ms/20 ms [14,24].

**Table 5.** Adding behavior of IT load with 4 MW PV.

Stage	$\Delta f$ threshold	IT load regulation ratio
1	+0.02 Hz	10%
2	+0.04 Hz	20%
3	+0.06 Hz	30%
4	+0.08 Hz	40%
5	+0.1 Hz	50%
6	+0.12 Hz	60%

**Table 6.** Adding behavior of cooling loads with 4 MW PV.

Stage	$\Delta f$ threshold	Cooling load regulation ratio
1	+0.14 Hz	10%
2	+0.16 Hz	20%
3	+0.18 Hz	30%
4	+0.2 Hz	40%
5	+0.22 Hz	50%
6	+0.24 Hz	60%
7	+0.26 Hz	70%
8	+0.28 Hz	80%
9	+0.3 Hz	90%
10	+0.32 Hz	100%

#### 4. Case study

In order to evaluate effectiveness of the proposed load control strategy, numerical experiments via MATLAB/Simulink are performed to simulate various operation statuses of a data center microgrid. This microgrid consists of two 2 MW diesel generators, one PV generator, one cooling system, and 10 IT clusters (including one storage cluster, two processing clusters, and seven computing clusters) with 0.2 MW power consumption each. Each IT cluster is connected to the data center microgrid bus through UPS. The PUE for data center is set at 2. Parameters of cooling loads (including fan, CRAH, and chiller) are set according to [16].

The following three cases are studied in a 16-second time period to evaluate effectiveness of the proposed control approach to regulating frequency of a data center microgrid in islanded mode. In all cases, PV power outputs are calculated with the temperature of solar panels set to 25°C.

**Case 1:** *Microgrid with 0.5 MW PV integration (12.5% penetration).* In this case, the irradiance of sunlight falls from 1000 W/m<sup>2</sup> at 7 s to 0 W/m<sup>2</sup> at 7.25 s and returns back to 1000 W/m<sup>2</sup> from 12 s to 12.25 s. This leads the power output of PV to drop from 0.5 MW to 0 MW, then return to 0.5 MW, as shown in Figure 8.

Figure 8 shows frequency, voltage magnitude, and power output of PV and two diesel generators

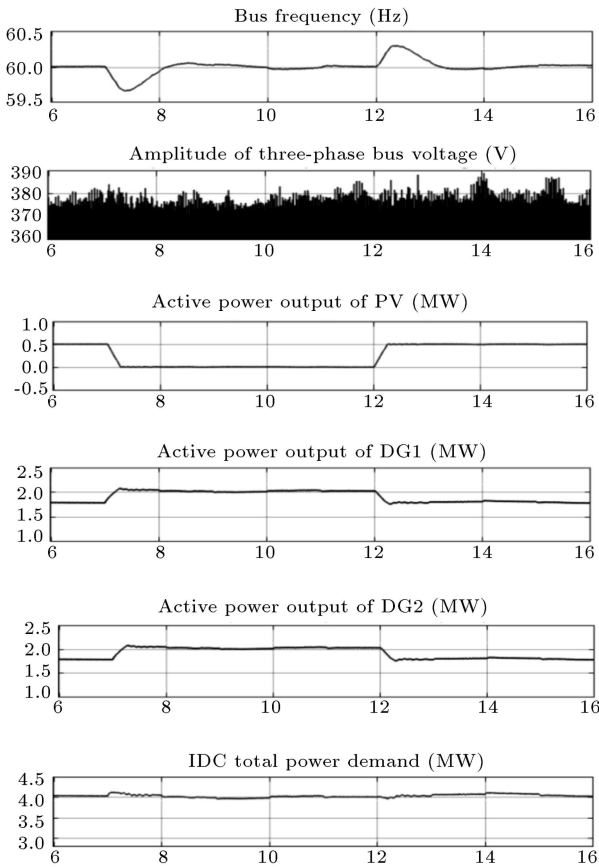


Figure 8. Frequency and voltage magnitude of the main bus of the microgrid, active power output of PV and DGs, and total power demand of data center in Case 1.

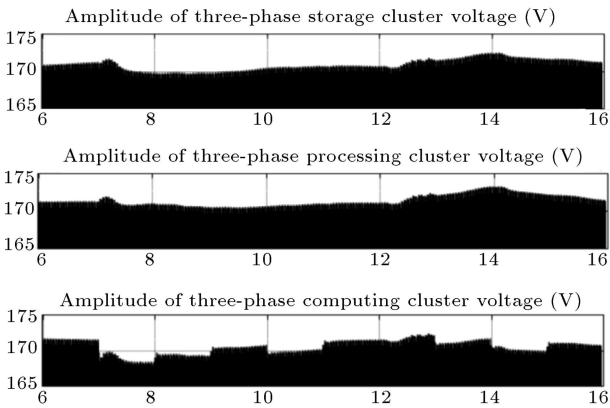


Figure 9. Terminal voltage of IT clusters.

as well as total power loads of the data center for the entire 16 seconds. We can observe in the figure that PV power output changes do not drive frequency out of the range [59.5 Hz, 60.5 Hz]. In addition, voltage magnitude varies between 375 V and 390 V, which is within the range of minimum voltage 372.4 V (i.e., 0.95\*392 V) and maximum voltage 411.6 V (i.e., 1.05\*392 V), corresponding to the desired 392 V level. Figure 9 further shows phase-to-ground terminal voltage magnitudes of the three phases for

the IT clusters. It shows that terminal voltages of IT clusters are not significantly affected by power output change of PV and they are kept close to the desired 170 V. This study shows that when the PV penetration level is not high, the fluctuation of PV power output may not bring significant frequency issue or other power quality concerns to the data center microgrid;

**Case 2: Microgrid with 1 MW PV integration (25% penetration).**

**Case 2.1: Primary frequency control without load controller.** In this case, the irradiance of sunlight falls from 1000 W/m<sup>2</sup> at 7 s to 0 W/m<sup>2</sup> at 7.25 s, which leads to the drop of the power output of PV from 4 MW to 0 MW, as shown in Figure 10. Figure 11 shows that the irradiance of sunlight rises from 0 W/m<sup>2</sup> at 12 s to 1000 W/m<sup>2</sup> at 12.25 s, which leads to increase in the power output of PV from 0 MW to 4 MW.

Figure 10 shows frequency and voltage magnitude of the main bus of the data center microgrid, active power output of PV and DGs, and total power demand of the data center. It illustrates that as power output

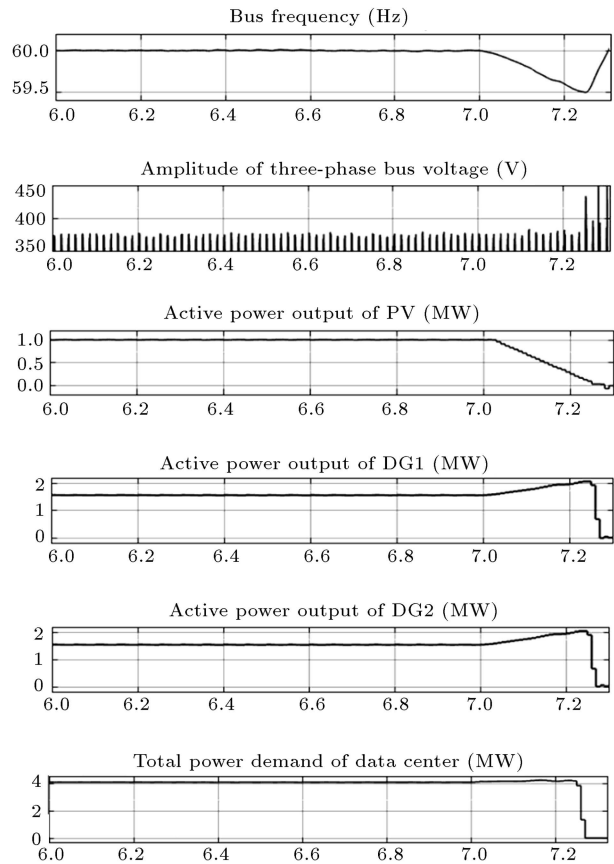
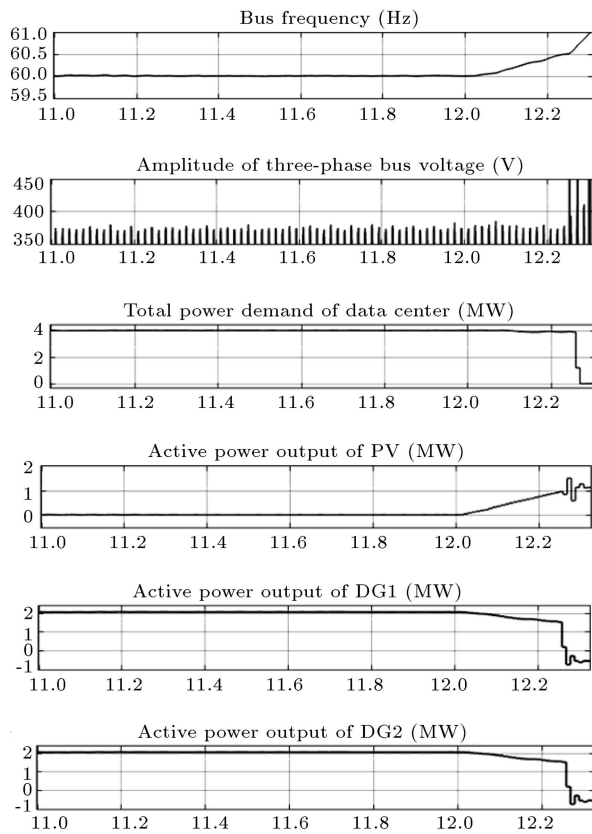


Figure 10. Frequency and voltage magnitude of the main bus of the microgrid, active power output of PV and DGs, and total power demand of data center in Case 2.1 from second 6 to second 7.2.



**Figure 11.** Frequency and voltage magnitude of the main bus of the microgrid, active power output of PV and DGs, and total power demand of data center in Case 2.1 from second 11 to second 12.2.

of PV decreases, frequency goes below 59.5 Hz and the under-frequency protection system of data center microgrid disconnects all UPSs and cooling systems to protect the physical assets. Although disconnected UPSs can temporarily maintain sustained power supply to IT equipment, this frequent (due to fluctuations of PV output) and unexpected discharging (not triggered by power outages) could significantly compromise lifetime of UPSs, which is not economical due to high cost of UPSs. Figure 11 further shows the same set of profiles when PV power output increases from 0 to 1 MW. This triggers the bus frequency to higher than 60.5 Hz. As a result, over-frequency protection system of data center microgrid disconnects all UPSs and the cooling system. Moreover, the bus frequency cannot be stabilized after disconnecting those assets. Such a frequency surge could damage diesel generators and transformers.

**Case 2.2:** *Primary frequency regulation with load controller.* In this case, besides two DGs, data center cooling system loads also participate in the frequency regulation based on our proposed control strategy. The power output of PV drops from 1 MW at 7 s to 0 MW at 7.25 s, and returns to 1 MW from 12 s to 12.25 s.

Figure 12 shows frequency and voltage magnitude

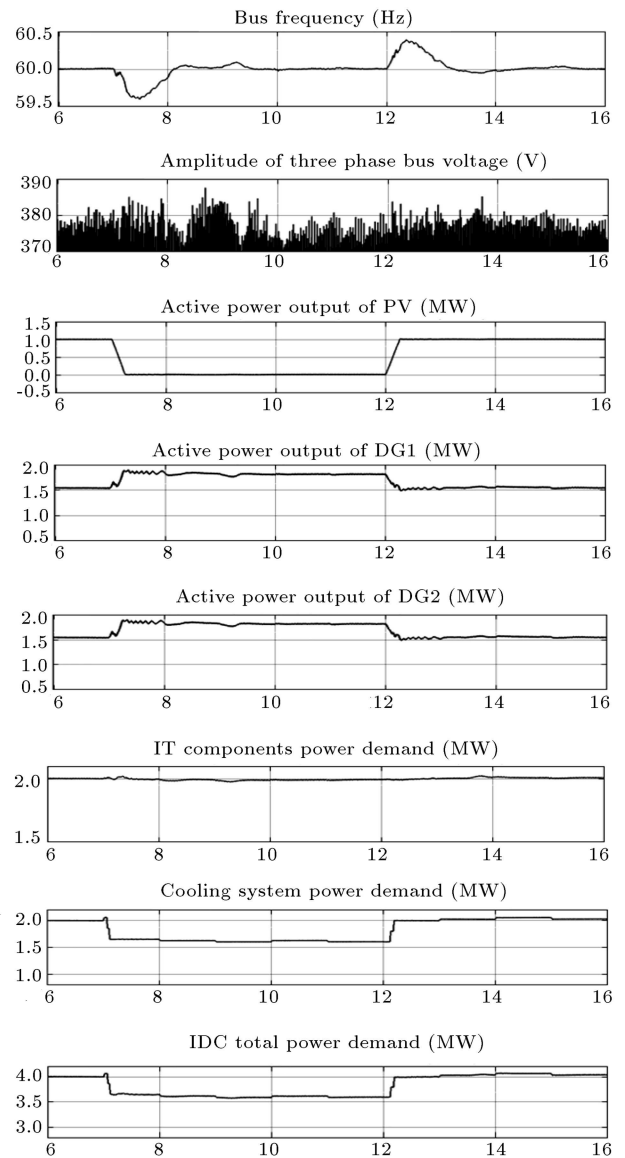


**Figure 12.** Frequency and voltage magnitude of the main bus of the microgrid, active power output of PV and DGs, and cooling system and total power demands of data center in Case 2.2.

of the main bus of the data center microgrid, active power output of PV and DGs, and cooling system and total power demands. It is evident that 0.4 MW cooling load is cut off around 7.25 s to pull frequency back to above 59.5 Hz. On the other hand, 0.4 MW cooling load is restored around 12.25 s to maintain frequency under 60.5 Hz. Thus, as load can be effectively controlled to provide frequency regulation, over- or under-frequency protection system is not activated. Figures 12 and 13 further illustrate that both bus voltage magnitude and terminal voltage of IT clusters are within the acceptable range.

**Case 3:** *Microgrid with 4 MW PV integration (100% penetration).*

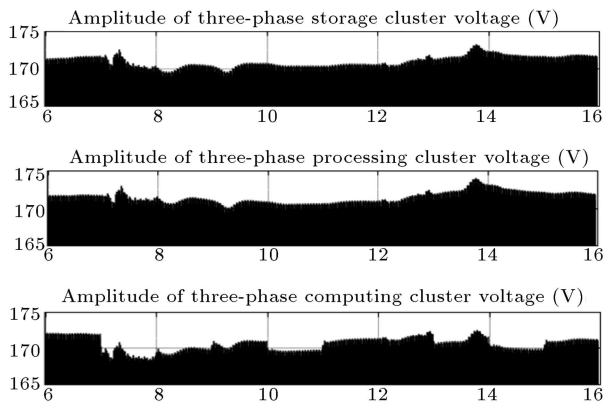


Figure 13. Terminal voltage of IT clusters.

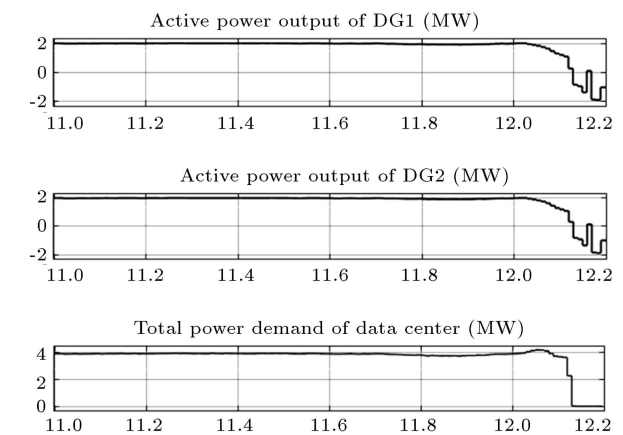
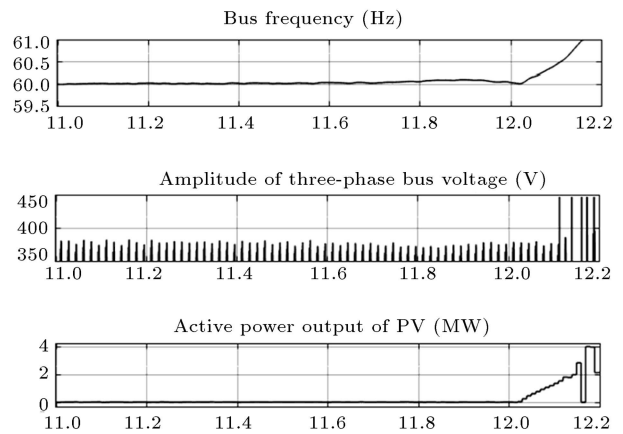


Figure 15. Frequency and voltage magnitude of the main bus of the microgrid, active power output of PV and DGs, and total power demand of data center in Case 3.1 from second 11 to second 12.2.

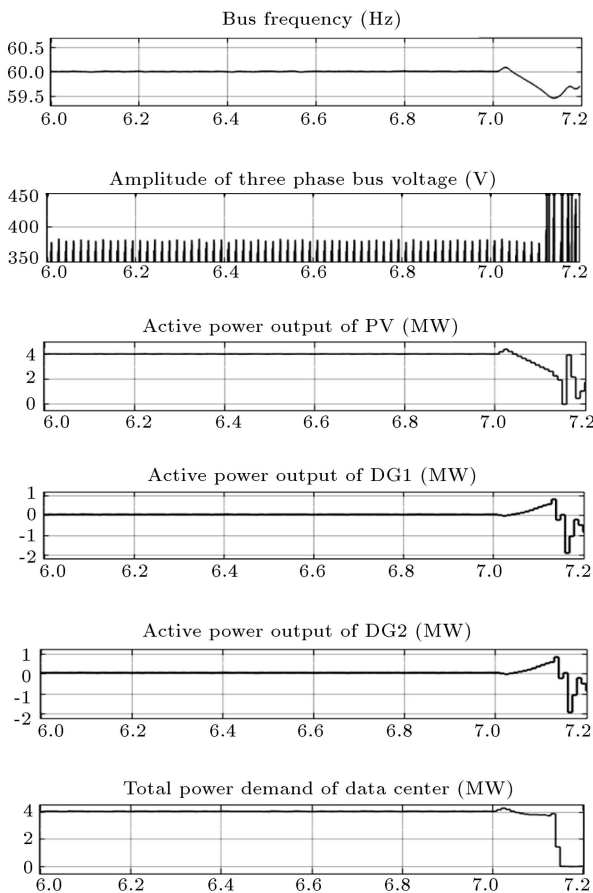


Figure 14. Frequency and voltage magnitude of the main bus of the microgrid, active power output of PV and DGs, and total power demand of data center in Case 3.1 from second 6 to second 7.2.

**Case 3.1.** *Primary frequency control without load controller.* In this case, the irradiance of sunlight falls from  $1000 \text{ W/m}^2$  at 7 s to  $0 \text{ W/m}^2$  at 7.25 s, which drops the power output of PV from 4 MW to 0 MW as shown in Figure 14. Figure 15 shows that irradiance of sunlight rises from  $0 \text{ W/m}^2$  at 12 s to  $1000 \text{ W/m}^2$  at 12.25 s, which raises the power output of PV from 0 MW to 4 MW.

The frequency and voltage magnitude of data center microgrid bus, active power output of PV and DGs, and total power demand of data center during the periods of 6-7.2 seconds and 11-12.2 seconds are shown in Figures 14 and 15. Same as for Case 2.1, the under-/over-frequency protection system disconnects all UPSs and the cooling system when the bus frequency goes below 59.5 Hz/above 60.5 Hz due to the sudden decrease/increase in PV generation. In addition, the entire microgrid system becomes unstable and frequency is unable to return to the nominal value.

**Case 3.2.** *Primary frequency regulation with load controller.* In this case, besides two DGs, data center (both cooling and IT) loads participate in the primary frequency regulation according to the proposed control strategy. The power output of PV drops from 4 MW at 7 s to 0 MW at 7.25 s, and rises back to 4 MW from 12 s to 12.25 s.

The frequency and voltage magnitude of data center microgrid bus, active power output of PV and DGs, and total power demand of data center are shown in Figure 16. It is illustrated that 2 MW cooling load is

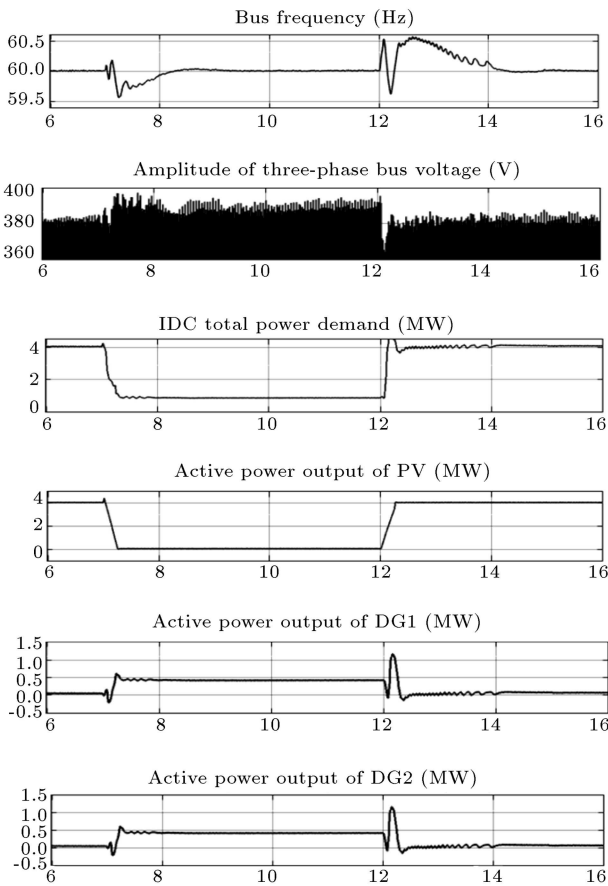


**Figure 16.** Frequency and voltage magnitude of the main bus of the microgrid, active power output of PV and DGs, and total power demand of data center in Case 3.2.

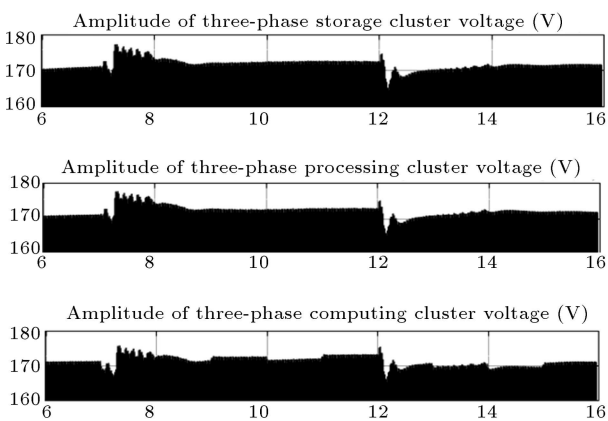


**Figure 17.** Terminal voltage of IT clusters.

cut off and the tasks of the 6 computing IT clusters are shifted out to recover frequency back to above 59.5 Hz when PV generation decreases from 4 MW to 0 MW. When PV generation increases from 0 MW to 4 MW, the tasks of 6 computing IT clusters are shifted in and 2 MW cooling load is restored to pull frequency under 60.5 Hz. Figures 16 and 17 further illustrate that both bus voltage magnitude and terminal voltage of IT clusters are within the acceptable range.

## 5. Conclusions

In this paper we presented a data center microgrid simulation model via MATLAB/Simulink, including traditional diesel generation units, PV generation, UPS, and power consumption model of data center (including IT components and cooling system), by considering characteristics of data center loads. A data center load control strategy was proposed for allowing data center loads to participate in the primary frequency regulation and then, it was verified by the microgrid simulation model. Numerical studies indicated that when the PV penetration was low, the sudden change in PV power output might not compromise microgrid frequency and consequently, load participation in the frequency regulation might not be critical. However, when the PV penetration was high (i.e., over 25% in our experiments), traditional generators were not able to maintain microgrid frequency within the required range and frequency regulation provided by data center loads became critical. Case studies clearly illustrated the importance of load control for providing frequency regulation in future green data centers with extremely high % PV penetration levels.

## References

1. Shehabi, A., Smith, S.J., Horner, N., et al., *United States Data Center Energy Usage Report*, Lawrence Berkeley National Laboratory, Berkeley, California, LBNL-1005775, p. 4 (2016).
2. Data Center Knowledge, 2014. [online] Available: <http://www.datacenterknowledge.com/archives/2014/12/17/undertaking-challenge-reduce-data-center-carbon-footprint/>
3. Li, J. and Qi, W. "Towards optimal operation of internet data center microgrid", *IEEE Transactions on Smart Grid*, **9**(2), pp. 971-979 (2018).
4. Yu, L., Tao, J., and Yulong, Z. "Distributed real-time energy management in data center microgrids", *IEEE Transactions on Smart Grid*, **9**(4), pp. 3748-3762 (2018).
5. Aksanli, B., Akyurek, A.S., and Rosing, T. "Minimizing the effects of data centers on microgrid stability", *Green Computing Conference and Sustainable Computing Conference (IGSC)*, 2015 Sixth International, pp. 1-9 (2015).
6. Chainer, T.J., Schultz, M.D., Parida, P.R., et al. "Improving data center energy efficiency with advanced thermal management", *IEEE Trans. Compon., Packag., Manuf. Technol.*, **7**(8), pp. 1228-1239 (2017).
7. Koch, B. and Slezak, D. "Less energy, more efficiency in server rooms and data centers", *Computer Science-Research and Development*, **33**(1-2), pp. 251-252 (2018).
8. Femia, N., Petrone, G., Spagnuolo, G., et al. "Optimization of perturb and observe maximum power

- point tracking method”, *IEEE trans. Power Electron.*, **20**(4), pp. 963-973 (2005).
9. Senjyu, T., Datta, M., Yona, A., et al. “A control method for small utility connected large pv system to reduce frequency deviation using a minimal-order observer”, *IEEE Transactions on Energy Conversion*, **24**(2), pp. 520-528 (2009).
  10. Han, H., Hou, X.C., Yang, J., et al. “Review of power sharing control strategies for islanding operation of ac microgrids”, *IEEE Trans. Smart Grid*, **7**(1), pp. 200-215 (2016).
  11. Che, L. and Shahidehpour, M. “DC microgrids: Economic operation and enhancement of resilience by hierarchical control”, *IEEE Trans. Smart Grid*, **5**(5), pp. 2517-2526 (2014).
  12. Zhao, Z., Yang, P., Xu, Z., et al. “Control strategy of energy storage system for frequency support of autonomous microgrid”, In *Electrical Machines and Systems (ICEMS), 2015 18th International Conference on*, pp. 422-426 (2015).
  13. Molina-García, A., Bouffard, F., Kirschen, D.S. “Decentralized demand side contribution to primary frequency control”, *IEEE Trans. on Power Syst.*, **26**(1), pp. 411-419 (2011).
  14. Pourmousavi, S. and Nehrir, M. “Real-time central demand response for primary frequency regulation in microgrids”, *IEEE Transactions on Smart Grid*, **3**(4), pp. 1988-1996 (2012).
  15. Medina, J., Muller, N., and Roytelman, I. “Demand response and distribution grid operations: Opportunities and challenges”, *IEEE Trans. on Smart Grid*, **1**(2), pp. 193-198 (2010).
  16. Dayarathna, M., Wen, Y., and Fan, R. “Data center energy consumption modeling: A survey”, *IEEE Communications Surveys & Tutorials*, **18**(1), pp. 732-794 (2015).
  17. ABB. “Review: data centers” (2013).
  18. Sawyer, R., *Calculating Total Power Requirements for Data Centers*, White Paper, American Power Conversion (2004).
  19. Chen, Z., Wu, L., and Li, Z. “Electric demand response management for distributed largescale internet data centers”, *IEEE Trans. on Smart Grid*, **5**(2), pp. 651-661 (2014).
  20. Meisner, D. and Wenisch, T.F. “Does low-power design imply energy efficiency for data centers?”, in Proc. 17th IEEE/ACM ISLPED, pp. 109-114 (2011).
  21. Pelley, S., Meisner, D., Wenisch, T.F., et al. “Understanding and abstracting total data center power”, In *Workshop on Energy Efficient Design* (2009).
  22. Sawyer, R., *Calculating Total Power Requirements for Data Centers*, White Paper, American Power Conversion (2004).
  23. Zhabelova, G., Yavarian, A., and Vyatkin, V. “Data center power dynamics within the settings of regional power grid”, *Emerging Technologies & Factory Automation (ETFA) 2015 IEEE 20th Conference on*, pp. 1-5 (2015).
  24. Bhattacharya, A.A., Culler, D., Kansal, A., et al. “The need for speed and stability in data center power capping”, in *Sustainable Computing: Informatics and Systems*, **3**(3), pp. 183-193 (2013).

## Biographies

**Wenbo Qi** received his BS degree in Wind Energy and Power Engineering and Master degree in Electrical Engineering from North China Electric Power University, Beijing, China, in 2010 and 2013, respectively, and PhD degree in Electrical Engineering from Clarkson University, NY, USA, in 2018. Presently, he is working as a power system developer in Open Systems International, Inc., Medina, Minnesota, USA. His research interests include green data center, demand response, and power system modelling.

**Jie Li** received her BS degree in Electrical Engineering and MS degree in Systems Engineering from Xi’an Jiaotong University, China, in 2003 and 2006, respectively, and PhD degree in Electrical Engineering from Illinois Institute of Technology, USA, in 2012. Presently, she is an Assistant Professor in the ECE Department at Rowan University. Before joining Rowan University, she worked with Clarkson University. Her research interests include green data center, demand response, and electricity market bidding strategy.